

The Kinetic Treatment of Space Plasmas

Joseph F. Lemaire and Viviane Pierrard

*Institut G. Lemaître, Université Cath. Louvain, & Institut d'Aéronomie spatiale de Belgique
3, Avenue Circulaire, B-1180 Brussels, Belgium*

Abstract. To describe transport in space plasmas hydrodynamic and kinetic approaches have been proposed and used. These approaches are appropriate for separate collisional regimes. Hydrodynamics is a valid approximation of the general transport equations in highly collision-dominated fluids. In low-density plasmas where the Knudsen number is larger than 1 like at high altitude in planetary and stellar exospheres, only a kinetic treatment is appropriate. Collisionless models of the high altitude planetary atmospheres have been first based on the solution of the Liouville-Vlasov equation. They proved to be very useful zero-order kinetic approximations since they have demonstrated the importance of the internal polarization electric field in the acceleration process of the solar wind and polar wind protons. Higher order kinetic approximations have been more recently developed. Numerical solutions of the Fokker-Planck equation for the velocity distribution of the electrons in the solar wind and H^+ ions in the polar wind have now been obtained. The major and key differences between the results of these different approaches are illustrated through solar wind and terrestrial polar wind applications with comparison of the particle velocity distribution functions found in the different models.

Application of the hydrodynamic equations to model the solar and polar winds

In the atmosphere of Earth and of other planets, as well as in planetary ionospheres or stellar coronae, there is always an altitude where the density is so low that Kn , the Knudsen number, becomes larger than unity. This level is called the exobase. The region above the exobase is called the exosphere. Exospheric models may there be considered as acceptable zero-order kinetic approximations. Below the exobase it is considered that the collision frequency is large enough to establish a nearly Maxwellian and isotropic velocity distribution function (VDF) over relatively short time scales, so that the Chapman-Enskog expansions of the VDF, and the (magneto-)hydrodynamic (MHD) equations are valid approximations of the mathematical theory of non-uniform gases. Between the collision-dominated region and the collisionless region there is a transition region where none of these extreme approximations are applicable. In the case of the polar wind, the transition region is located between 1500 km and 2500 km. In the solar corona the Knudsen number becomes equal to unity at about 6 (or 2) solar radii at equatorial (or polar) latitudes.

Parker in 1958 [1] as well as MHD modellers after him, applied various Euler and Navier-Stokes hydrodynamic equations, as well as Grad's moment approximations to model (with limited success) the supersonic expansion of the solar corona which was then called the solar wind. Parker's hydrodynamic solutions for the solar wind were however extended beyond the transition region into the collisionless exosphere, although inter-particle Coulomb collisions become so rare that $Kn > 1$: i.e. he applied a fluid-like description and approximation of the transport equations in a region where the validity conditions of the Chapman-Enskog or Grad expansions breakdown. But since some of the predictions of Parker's critical solution of the hydrodynamic equations had been soon confirmed (in 1961) by the observations of a supersonic solar wind plasma flow at 1 AU, the popularity of the hydrodynamic models of the solar wind had become overwhelming in the early 60's. This prompted Banks and Holzer [2] to apply, a decade later, these same hydrodynamic equations to model the terrestrial polar wind i.e. the flow of thermal ionospheric plasma out of the high latitude polar caps.

Kinetic models for the solar and polar winds

The validity of the hydrodynamic approximations used in the collisionless part of the solar corona and of polar ionosphere was soon questioned and challenged first by Chamberlain (1960) [3] in the case of the solar wind, and later by Dessler and Cloutier (1969) [4] in the case of the polar wind. These authors proposed to use, instead, exospheric models similar to those proposed a long time ago by Jeans in his study of the escape of neutral atoms from planetary atmospheres. Similar exospheric models had also been proposed in the early 60's by Brandt-Chamberlain and by Opik-Singer to model the neutral exospheric density distribution of the geocorona. The history of the development of these exospheric models can be found in several reviews [5,6,7,8].

The basic differences between MHD and exospheric models are illustrated on Figure 1 presenting the isocontours of the solar wind electrons VDF obtained at three different radial distances. A collisionless exospheric VDF is illustrated on the r.h.s., and the VDF associated to the hydrodynamic 5-moments approximation is given on the l.h.s. The latter is a drifting-maxwellian with the same drift speed (first order moment of the VDF) and density (zero-order moment of the VDF) as the exospheric VDF.

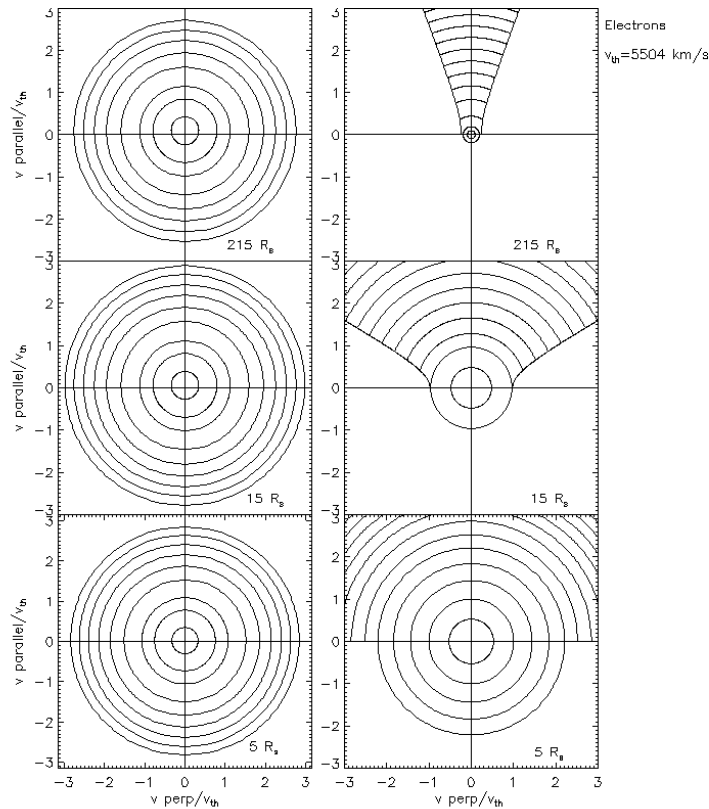


FIGURE 1. Comparison of the solar wind electrons VDF obtained at three different radial distances (i) for the fluid/hydrodynamic 5-moments approximation (left), and (ii) for a purely exospheric model (right).

The bulk speed around 500 km/s in the vicinity of the Earth's orbit ($215 R_s$) is given in the top panels. This average velocity is small compared to the thermal speed of the electrons ($v_{th}=5504$ km/s in this example). The coronal temperature is $T=10^6$ K at $5 R_s$ so that the peak of the VDF in the fluid approximation is relatively close to the origin ($v_{parallel}/v_{th}=0$, $v_{perp}/v_{th}=0$) in all l.h.s. panels of Fig. 1. Contrasting differences between the two model VDFs are outstanding: in both models the VDF has a vertical asymmetry but in the exospheric model, the velocity distribution function of the particles is asymmetric only at higher energies i.e. for suprathermal particles on escaping orbits. Only electrons with a large enough velocity contribute to the net radial flux of particles as well as to the flux of energy. Ballistic and trapped particles with lower velocities have a symmetric distribution and contribute to the density and pressure but not to the flux of particles neither the energy flux. Due to the assumed conservation of the magnetic moment of charged particles spiralling around the interplanetary magnetic field lines, the VDF is focussed in the outward direction parallel to the magnetic field lines, which are assumed to be radial in this exospheric or zero-order kinetic model of the solar wind.

Unlike in Chamberlain's kinetic model for the coronal evaporation, a rather satisfactory agreement was obtained by Lemaire and Scherer (1971) [9] between the results of their exospheric model and the average solar wind measurements at 1 AU in the ecliptic plane in low speed solar wind regimes. This better agreement must be attributed to the more appropriate and correct choice for the polarization electric field, instead of the Pannekoek-Rosseland electric field postulated in Chamberlain's solar breeze exospheric model.

The upward electric field is larger, and large enough to accelerate the protons out of the gravitational well. In Lemaire and Scherer's exospheric models the electrostatic potential difference between the exobase and infinity is of the order of 700 V which is much larger than that of the Pannekoek-Rosseland electric field (150 V). A value of 700 V is required to reduce the net thermal escape flux of the electrons in order to be precisely equal to the outward flux of protons.

Although the temperature averaged over all angles are satisfactorily predicted in these exospheric models, the temperature anisotropies are however much larger than observed. Lemaire and Scherer argued that Coulomb collisions would reduce the too large theoretical temperature anisotropies without changing significantly the average energies or average temperatures of the escaping electrons and ions. This indicates the need for post-exospheric kinetic approximations taking into account pitch angle scattering by Coulomb collisions.

Figure 2 presents the isocontours of the velocity distribution function for the solar wind protons calculated at three different radial distances in an exospheric model (r.h.s.), as well as for a 5-moments hydrodynamic approximation (l.h.s.). Since the mass of the protons is 1832 times larger than that of the electrons, their thermal speed is much lower than that of the electrons. As a consequence, the displacement velocity or bulk velocity of the protons is more clearly apparent in the hydrodynamic model than in Fig. 1.

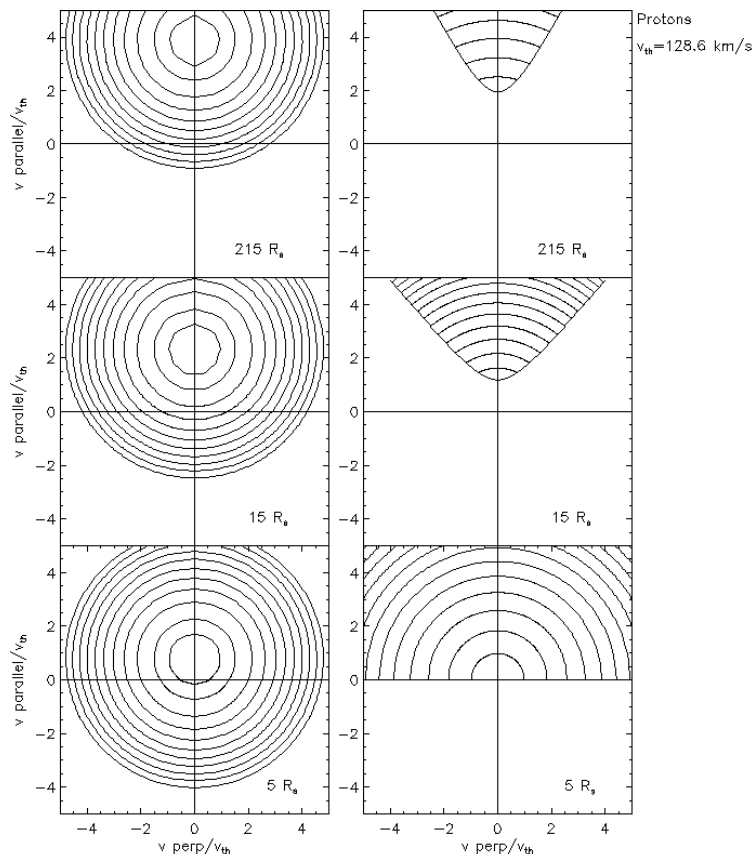


FIGURE 2. Comparison of isocontours of solar wind protons VDF obtained with the 5-moments hydrodynamic approximation (left) and with a purely exospheric model (right) at three different radial distances.

Due to the large electrostatic potential (700 V), the protons are accelerated outwards to a bulk velocity of the order of 300 km/s at 1 AU, since they are in a large repulsive electric potential distribution. Indeed, the repulsive electrostatic potential energy distribution of the protons is larger than the attractive gravitational potential energy. Outward accelerated protons are unable to come back to the Sun; this is why the downward part of the proton VDF is empty at the 5 R_s exobase level as well as at any other exospheric altitudes. Therefore, the VDF is truncated in the exospheric model and looks rather artificial and unrealistic. Nevertheless, this zero-order kinetic approximation gives moments in quite reasonable agreement with the observations at 1 AU [9].

The main achievement of this exospheric approach over the hydrodynamic ones, has been to explain in a simple and straightforward physical manner the origin of the upward directed parallel electric field that accelerates to supersonic velocities the thermal ions of the solar corona and polar ionosphere. The kinetic approach clearly shows how to calculate this polarization E-field to keep the electron density equal to the total ion density, everywhere in the exosphere. It outlines also how to determine the field-aligned electrostatic potential between the exobase altitude and infinity in order to reduce the large evaporation flux of the thermal electrons, and force it to be precisely equal to the Jeans escape flux of the thermal protons accelerated out of the solar corona and polar ionosphere.

Enhanced non-maxwellian tails in the electron VDF (simulated with Lorentzian VDFs) contribute to increase to even higher values the bulk velocity of the solar wind and polar winds observed at large distances in fast speed streams [10]. This is illustrated on Fig. 3 showing the number density of the solar wind particles, the electrostatic potential, the bulk speed and the total potential of the protons as a function of the altitude (in solar radii) in three different exospheric models. In the first model the VDF of the electrons is assumed to be a truncated maxwellian at the exobase altitude located at $5 R_s$ (thick line above $5 R_s$). In the second model the VDF is a truncated Lorentzian ($\kappa=3$) with identical exobase conditions (thin line above $5 R_s$). The bulk velocity at large radial distance is clearly larger in the Lorentzian model than in the Maxwellian one. Enhanced suprathermal tails in non-maxwellian VDFs for coronal electrons, as assumed in this exospheric model developed by Maksimovic et al. [11], are responsible for larger field aligned electric potential that can accelerate the protons to larger bulk speeds at 1 AU.

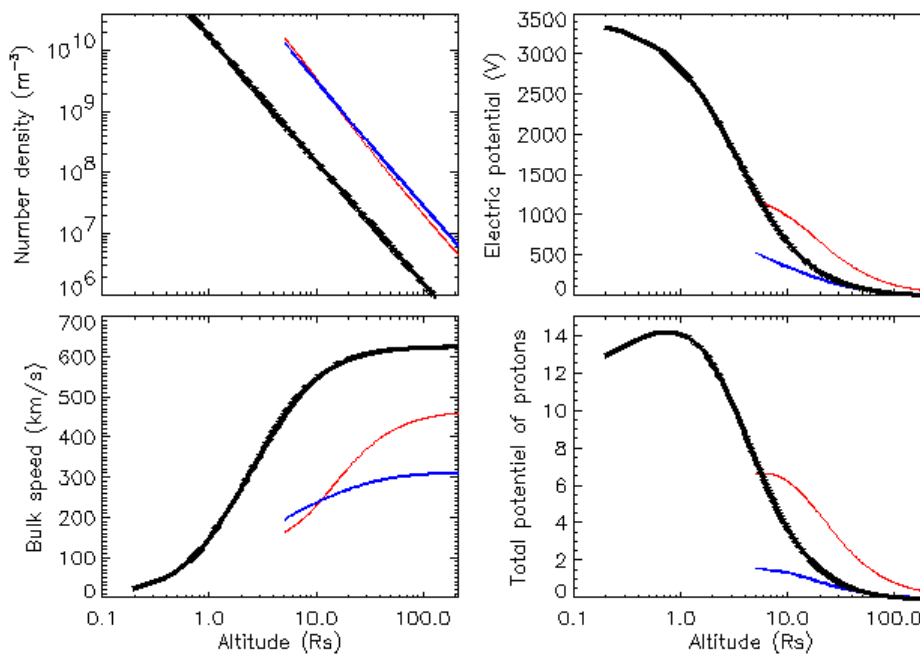


FIGURE 3. Number density (upper left panel), electrostatic potential (upper right panel), bulk speed (lower left panel) and total potential (lower right panel) of the solar wind protons as a function of the altitude above the photosphere for three different exospheric models. The first one is obtained with a Maxwellian VDF (thick lines above $5 R_s$), the second with a Lorentzian VDF with $\kappa=3$ (thin lines above $5 R_s$). The exobase altitude is located at $5 R_s$ in these two models. The bold lines starting at a heliospheric altitude of $0.1 R_s$ presents the results for a Lorentzian exospheric model with $\kappa=3$ but for an exobase altitude at $0.1 R_s$.

The boldest lines correspond to an exospheric model for which the exobase altitude is only $0.1 R_s$ as expected in low-density coronal holes. The gravitational potential barrier limiting the net escape flux of protons out of coronal holes tends to increase the electric potential difference. As a consequence, the solar wind velocity at large distances is enhanced to even higher bulk velocities [12]. Thus a lower altitude of the exobase (e.g. at $0.1 R_s$) drives the bulk velocity up to much larger values at 1 AU. This supports the observations indicating that the fastest solar wind streams originate in low-density coronal holes.

Nevertheless exospheric models are based on extreme assumptions: the complete absence of collisions above the exobase altitude. Therefore, they should be viewed only as zero-order kinetic approximations. To build higher order kinetic approximations and therefore more realistic VDF of space plasmas, it is necessary to calculate numerical solutions of the Fokker-Planck equation instead of the collisionless Vlasov equation. Pierrard and Lemaire (1998) [13] and Pierrard et al. (1999, 2001) [14,15] have developed such post-exospheric collisional kinetic models for the polar wind and for the solar wind. Figure 4 presents the VDF of the solar wind electrons found by solving the Fokker-Planck equation in the transition region between 2 and 13 solar radii. Due to the assumed topside boundary conditions the VDF is anisotropic in the collisionless region. Note that the isocontours are now smoother than in the purely exospheric model where the distribution was sharply truncated as shown in the r.h.s. panels of Fig. 1; there are however striking similarities. The kinetic solution illustrated in Fig. 4 is a 10×10 polynomial expansion of the electron VDF in terms of 10 Legendre polynomials in $\cos \theta$ (where θ is the angle between the velocity and the radial direction), and 10 speed polynomials in velocity (see [16] for the definition of speed polynomials).

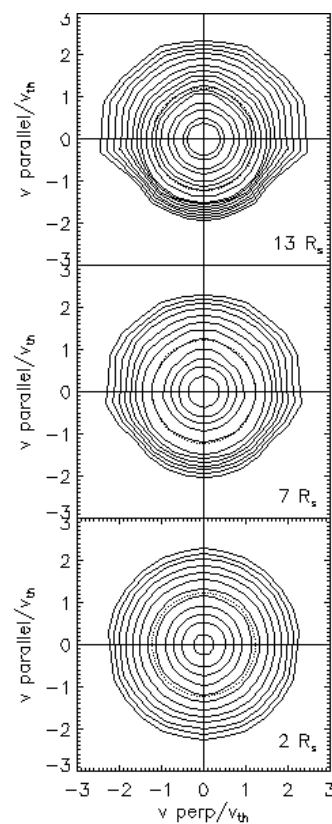


FIGURE 4. Isocontours of the solar wind electrons VDF found by solving the Fokker-Planck equation in the transition region between 2 and 13 solar radii [15].

For both kinetic models of the solar wind (the exospheric one in Fig. 1, as well as for the post-exospheric models in Fig. 4) the lower energy electrons in the vicinity of $v=0$ have a symmetric VDF with respect to the horizontal plane. These electrons are ballistic and collision-dominated particles; they do not contribute to the net fluxes of electrons in the solar and polar winds unlike in the hydrodynamical model illustrated in the l.h.s. panels of Fig. 1.

In the polar wind transition region, the solution of the Fokker-Planck equation for the H^+ ions is a VDF that changes even more drastically and in a more spectacular manner from a nearly isotropic maxwellian in the low altitude collision dominated region, to a doubly peaked function at high altitudes [17]. The isocontours of the polar wind protons are illustrated on Fig. 5 for three different altitudes in the transition region. The electrostatic potential distribution induced by the gravitational charge separation between the dominating background oxygen ions and the electrons accelerates the terrestrial hydrogen ions upward to supersonic velocities along the open polar cap magnetic field lines.

Only suprathermal protons contribute to the net upward flux, while the lower energy thermal protons experience more frequently Coulomb collisions with the background oxygen ions; the latter H^+ ions form the peak located around the origin in the $(v_{\text{parallel}}, v_{\text{perp}})$ velocity space. The VDF around this low energy peak tends toward an isotropic maxwellian VDF with zero displacement velocity in the vertical direction. This is a key difference between this kinetic VDF and that associated with hydrodynamic models illustrated in the l.h.s of Figs. 1 and 2. In these latter cases the peak of the VDF has a non zero displacement velocity whose value increases gradually with altitude. In hydrodynamic models the VDF is asymmetric at the origin and the low energy particles contribute to the upward fluxes of particles and energy.

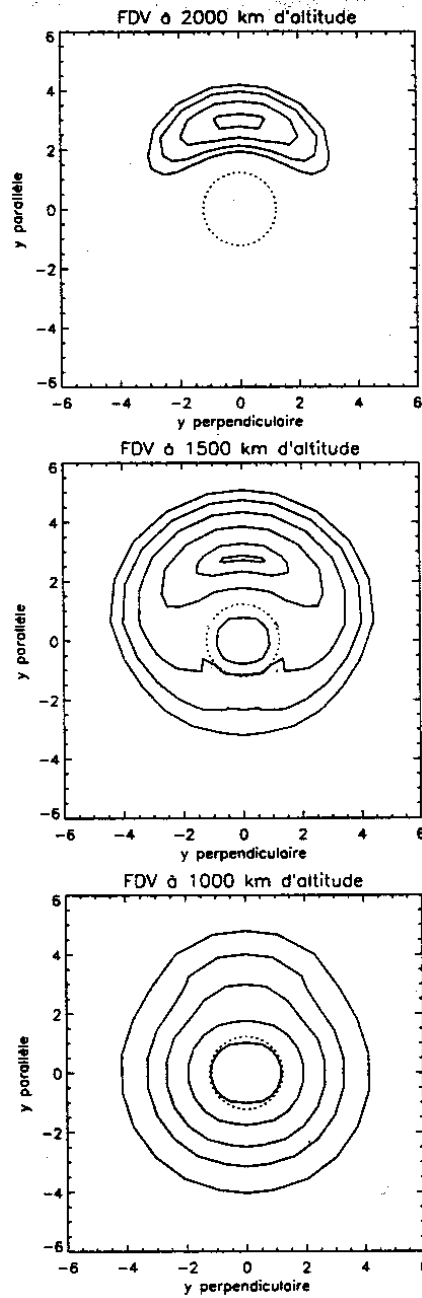


FIGURE 5. Velocity distribution function of the terrestrial H^+ polar wind ions at 3 different altitudes in the transition region [17].

Doubly-peaked VDF similar to those presented on Fig. 5 have also been obtained by Direct Simulation Monte Carlo (DSMC) for H^+ ions in the polar wind flow [18]. These DSMC solutions confirm that kinetic (exospheric or Fokker-Planck) solutions are fundamentally different from the VDF associated with the solutions of 5 or 8-moment hydrodynamic equations [19], or of any other set of hydrodynamic equations that proceed from the Grad or Chapman-Enskog expansion of the VDF.

The Grad and Chapman-Enskog mathematical theories are widely recognized as providing valid expansions for the VDF $f(\mathbf{v}, t)$, at least (i) when the average collision time is much smaller than the characteristic time of evolution for the $f(\mathbf{v}, t)$, and (ii) when/where the mean free path of the particles is much smaller than the characteristic scale length over which the bulk velocity \mathbf{u} , the number density n or the temperature T characterizing the dispersion of the VDF change significantly (i.e. when/where the corresponding Knudsen numbers, Kn , are all much smaller than unity). Laboratory measurements of acoustic wave dissipation and propagation speed have confirmed that under these standard conditions ($Kn \ll 1$). $f^{(2)}(\mathbf{v}, t)$ and $f^{(1)}(\mathbf{v}, t)$, the second and first approximations of the VDF, already fit very well the experimental results. Nevertheless, this good agreement should not qualify these hydrodynamic approaches for being infallible and justifiable in all cases: e.g. when the Knudsen number becomes larger than unity.

The hydrodynamic approximations, the hierarchy of transport equations and their associated expansions of velocity distribution functions are of course useful approximations in the lower altitude regions of solar wind, polar wind and more generally in space plasmas where the mean free path of the electrons and ions is much smaller than the characteristic scale length of the density distributions, over a wide range of energies. But in the collisionless region where the Knudsen number for particles of mean thermal energies and suprathermal energies is much larger than unity, kinetic equations must be solved to determine the spatio-temporal evolution for the microscopic VDF of the collisionless neutral atoms, ions and electrons. In these exospheric regions the usual Fourier law ($q = -\lambda \text{grad } T$) and the Navier-Stokes expressions for the components of the pressure tensors fail to be applicable. The Onsager relations of ordinary thermodynamics are then also out of order.

In the transition region where the Knudsen number increases from less than 0.1 to over 10, Boltzmann or Fokker-Planck type of equations have to be solved to determine how the VDFs transform from a one peak nearly isotropic and nearly maxwellian distribution functions, to any non-maxwellian and anisotropic functions like that illustrated in Fig. 5 for H^+ ions in the polar wind.

In the transition region between the collision-dominated and collisionless regions the first order approximation of the VDFs does not fit a displaced maxwellian with a gradually increasing displacement velocity as a function of altitude, like that illustrated in the l.h.s. panels of Fig. 1 and 2. In kinetic solutions of the VDF, the vertical displacement velocity of the low energy particles averages to zero, while only the suprathermal particles contribute effectively to the net fluxes of particles, energy and to any higher order odd moment of the VDF.

The kinetic solution for the VDF of atoms, ions and electrons evaporating from the topside of planetary or stellar atmospheres, resembles in some way to the distribution function of photons escaping from a stellar atmosphere: it is almost an isotropic Planck distribution in the lower region where local thermodynamic equilibrium (LTE) is satisfied; a non-LTE and anisotropic line spectrum with absorptions and emission lines being the dominant features of the spectra at higher altitudes where the optical depth (the analog of the Knudsen number for the particles) becomes smaller than unity.

Conclusions

Contrary to rather popular believe, hydrodynamic and kinetic approximations should neither be opposed, nor are they controversial, they must be regarded as complementary. Chapman-Enskog and alike expansions of the velocity distribution function are satisfactory approximations in the low altitude regions where $Kn < 0.1$ over a wide range of particle energies but the hydrodynamic approaches are not justifiable in exospheres where $Kn > 1$ for a wider and wider range of energies. It is often argued by the hydrodynamists that wave-particle interactions may replace Coulomb collisions in the exosphere. But this is a quite arbitrary and unproven statement, since there is no yet evidence that the waves and their intensity spectrum and type of polarization assumed in the exosphere are adequate to produce precisely the same diffusion in velocity space as Coulomb particle-particle interactions. In the collisionless region, exospheric models have been developed. They demonstrated the importance of the polarization electric field to accelerate the protons out of the gravitational potential well. Indeed, a correct and self-consistent evaluation of the charge separation electric field distribution in the solar corona and in the topside polar ionosphere leads to supersonic solar and polar wind flows comparable to those observed and initially modelled in terms of hydrodynamic models.

In the collisionless region, only particles with sufficient energy to escape or evaporate out of the corona can contribute to the outward flux of particles and to the energy flux. Ballistic and trapped particles have a symmetric velocity distribution and contribute to all even moments of the VDF (density, pressure, ...) but cannot contribute to the odd moments (net escape flux of particles, energy flux, ...). The kinetic velocity distribution functions are asymmetric but their asymmetry is fundamentally different from a displaced Maxwellian implicitly assumed in all hydrodynamic approaches. We view this a key difference between the exospheric or in general kinetic VDFs, and those postulated in the Chapman-Enskog theory, Grad or other mathematical theory of non-uniform gases. Exospheric solutions should be considered as a useful zero-order kinetic approximation. Post-exospheric models based on the solution of the Fokker-Planck equation are of course necessary to obtain higher order approximations in the region where $0.1 < Kn < 10$. Furthermore, to take into account distant backscattering collisions, it would be necessary to solve the Boltzmann equation or Fokker-Planck equation with additional non-local collision terms. But this is the next step which is far beyond the grasp in current modelling efforts of planetary and stellar exospheres.

ACKNOWLEDGMENTS

V. Pierrard wishes to thank the Belgian FNRS for the grant FC 36556.

REFERENCES

1. Parker, E.N., *Astrophys. J.*, **128**, 664 (1958).
2. Banks, P.M., and Holzer, T.E., *J. Geophys. Res.*, **73**, 6846 (1968).
3. Chamberlain, J.W., *Astrophys. J.*, **131**, 47 (1960).
4. Dessler, A.J., and Cloutier, P.A., *J. Geophys. Res.*, **74**, 3730 (1969).
5. Lemaire, J., and Scherer, M., *Rev. Geophys. Space Phys.*, **11**, 427-468 (1973).
6. Fahr, H.J., and Shizgal, B., *Reviews Geophys. Space Physics*, **21**, 75 (1983).
7. Shizgal, B., and Arkos, G. G., *Rev. Geophys.*, **34**, 4, 483-505 (1996).
8. Lemaire, J., and Pierrard, V., *Astrophys. and Space Science*, **277**, 169-180 (2001).
9. Lemaire, J., and Scherer, M., *J. Geophys. Res.*, **31**, 7479 (1971).
10. Pierrard, V., and Lemaire, J.F., *J. Geophys. Res.*, **101**, 7923-7934 (1996).
11. Maksimovic, M., Pierrard, V., and Lemaire, J., *Astron. Astrophys.*, **324**, 725-734 (1997).
12. Lamy, H., Pierrard, V., Maksimovic, M., and Lemaire, J.F., submitted to *J. Geophys. Res.* (2002).
13. Pierrard, V., and Lemaire, J., *J. Geophys. Res.*, **103**, 11701-11709, 1998.
14. Pierrard, V., Maksimovic, M., and Lemaire, J., *J. Geophys. Res.*, **104**, 17021-17032, (1999).
15. Pierrard, V., Maksimovic, M., and Lemaire, J., *J. Geophys. Res.*, **107**, 29305-29312 (2001).
16. Shizgal, B., and Blackmore, R., *J. Comput. Phys.*, **55**, 313-327 (1984).
17. Pierrard, V., *Ph.D. Thesis*, Univ. cath. Louvain (1997).
18. Barghouthi, A.R., Pierrard V., Barakat A. R., and Lemaire, J., *Astrophys. Sp. Sci.*, **277**, 427-436 (2001).
19. Lie-Svendsen, O., and Rees, M.H., *J. Geophys. Res.*, **101**, 2415-2433 (1996).